

# Combined temperature and RI sensor for exploring the phase transitions of ethanol solutions

Markus Solberg Wahl<sup>a</sup>, Øivind Wilhelmsen<sup>a,b</sup>, Dag Roar Hjelme<sup>a</sup>

<sup>a</sup>Norwegian University of Science and Technology (Norway)

<sup>b</sup>SINTEF Energy Research (Norway)

markus.s.wahl@ntnu.no

**Abstract:** A fiber optic interferometer based on core diameter mismatch is used in reflection mode to study the behavior of ethanol solutions with regards to concentration dependent thermal properties and phase transitions. A method to simultaneously measure both temperature and ethanol concentration in systems with non-linear sensitivities has been developed and characterized. © 2018 The Author(s)

**OCIS codes:** 060.2370 Fiber optics sensors; 120.3180 Interferometry.

## 1. Introduction

To detect the onset of a phase transition is very interesting both industrially, when tight process control is important, but also for research purposes. Heterogeneous nucleation is the dominant mechanism when water freezes, but the parameters involved are not well understood [1]. A sensor that can detect the phase transition and the temperature at which it occurs is therefore of interest.

Many different geometries have been explored to create modal fiber interferometers that are sensitive to the refractive index (RI) surrounding the sensor. For all of them a core mismatch that causes cladding modes to be excited, either through a waist-enlarged bitaper [2], sections of multi-mode (MM) fiber [3], coreless fiber [4], or with a thin-core fiber [5,6], the method in this work. These types of sensors have attracted a lot of attention due to their simplicity of both fabrication and operation, in addition to the general advantages of fiber optic sensors.

Common to the above-mentioned sensors is the inherent cross-sensitivity to temperature. Previous efforts to extricate the two parameters are dependent on constant sensitivities to create a linear set of equations that can be inverted [3,7]. As this is not always the case a more versatile method is presented here.

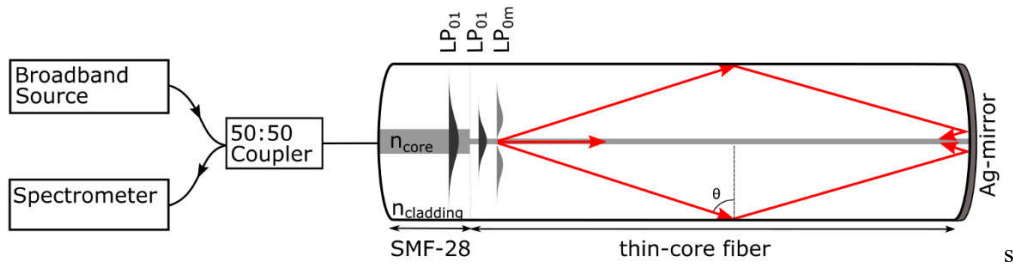
## 2. Design and principle

Figure 1 shows the measurement setup and the sensor schematic. The sensor is fabricated by splicing a 19 mm section of thin-core fiber (SM400) to the end of a single-mode fiber (SMF-28). The mismatch in diameter between the cores causes cladding modes to be excited, which interferes with the light still guided by the core. With circular cross sections and step-index profiles in both fibers, the excited cladding modes should only be linearly polarized radial modes i.e. LP<sub>0m</sub>, where *m* is a positive integer. Because the cladding modes are sensitive to the surrounding medium, the interference becomes a function of the refractive index (RI). Destructive interference between the core mode and the *m*th cladding mode will occur when the difference in optical path length (OPL) is equal to an odd number of  $\pi$ .

$$2\pi[n_{eff}^{core}(\lambda) - n_{eff}^{cladding,m}(\lambda, n_{ext})] \frac{L}{\lambda_{dip}} = (2n + 1)\pi \quad (1)$$

The equation neglects interference between cladding modes – a reasonable assumption if the amplitude of excited cladding modes is small compared to the core mode. It is also expected that the difference in effective RI between the core mode and a cladding mode is greater than the difference between two cladding modes. The period between two resonance dips caused by two cladding modes will therefore be larger than that between the core mode and a cladding mode. A given wavelength range should therefore be dominated by Equation 1.

The temperature sensitivity stems from the thermal expansion and thermo-optic response of the fiber material, as well as the thermo-optic coefficient of the surrounding medium [8]. Figure 2 shows the reflection spectrum with the two dips that are used throughout this study. Increasing the RI and temperature will both shift the spectrum to longer wavelengths, but with different sensitivities. A phase transition will cause a sudden change in RI as solids form on the fiber surface, and can hence be detected accordingly.



**Figure 1** Schematic of the sensor system. A superluminescent diode centered at 1550 nm, a single-mode coupler and a spectrometer with an optical resolution of 0.33 nm. The core-size mismatch creates surface sensitive cladding modes, while some light remains guided by the core.

The reflection-based geometry enables easy insertion of the probe into any system, while the independent read-out of temperature and RI enables simultaneous two-parameter operation. The mirror was fabricated by reducing silver through the mirror reaction [9], a simple and cheap method compared to the dry deposition methods normally used [4,5].

The experiments are performed in test tubes immersed in a silicon oil temperature bath, set at a cooling rate of 0.2 °C/min. With the sensor placed in the test tube containing various ethanol solutions no hysteresis was observed upon reheating, and it was concluded that the cooling rate was sufficiently slow.

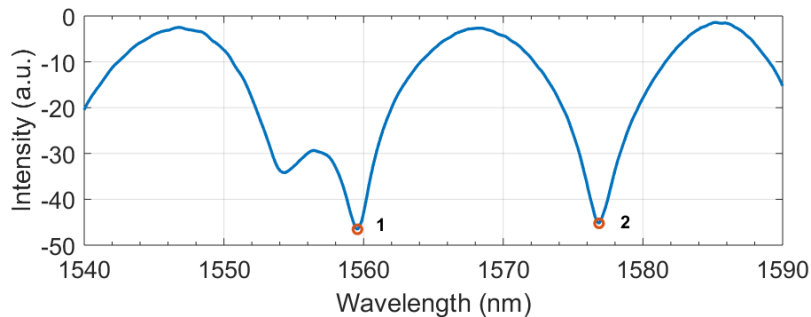


**Figure 2** Measured reflection spectrum in 25% ethanol at 15°C, with the two identified dips.

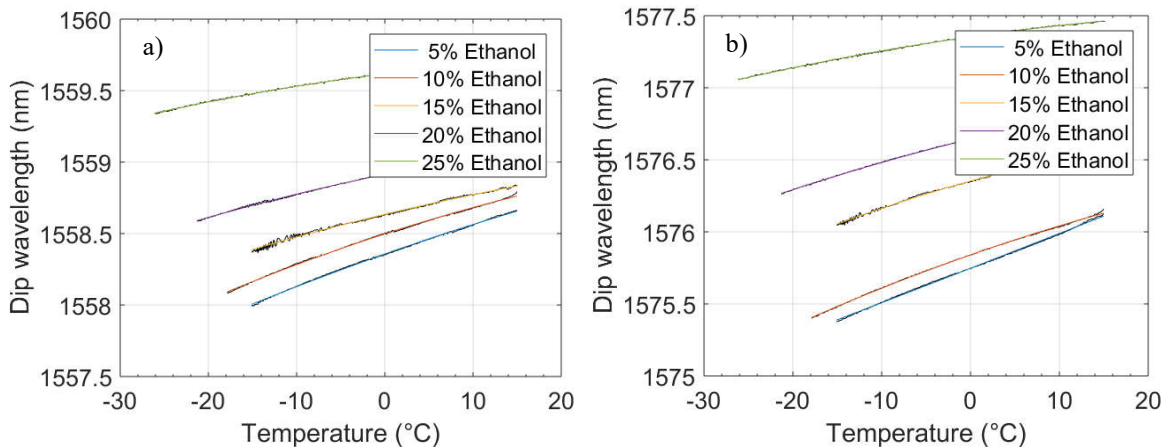


**Figure 3** Sensor response to temperature and ethanol concentration for dip 1 and 2 (a and b). Temperature was controlled with a temperature bath (0.2 °C/min) and measured with a Pt100 sensor.

### 3. Results

The thermal response of the sensor has been measured in different concentrations of ethanol, from 15°C down to the freezing point of the solution. The two dips that were tracked are shown in Figure 3 (a and b), which shows the slightly non-linear temperature sensitivity. Interestingly, the two peaks respond differently to both temperature and ethanol concentration, which forms the basis of the analytical method presented below. As the sensitivity to ethanol concentration is a direct result of the RI sensitivity, the method can be converted to measure RI.

Figure 4 shows the response to temperature and ethanol concentration in more detail. A surface fit described by 4<sup>th</sup> degree polynomials in both x- and y-directions, was found to the measured data (white lines) to create a two-dimensional calibration curve. A measured dip wavelength will in each plot correspond to a set of temperatures and ethanol concentrations, due to the cross-sensitivity. However, because the two dips behave

differently, two sets of possible temperatures and ethanol concentrations are found, from which one unique match can be extracted. This is shown in Figure 5, where the intersection between the two lines shows the measured temperature and ethanol concentration.

The measurements were found to be sensitive to bending in both the excitation fiber and detection fiber, which had to be stabilized. This could be a polarization sensitivity that potentially shows that the  $LP_{0m}$ -assumption is not entirely accurate.

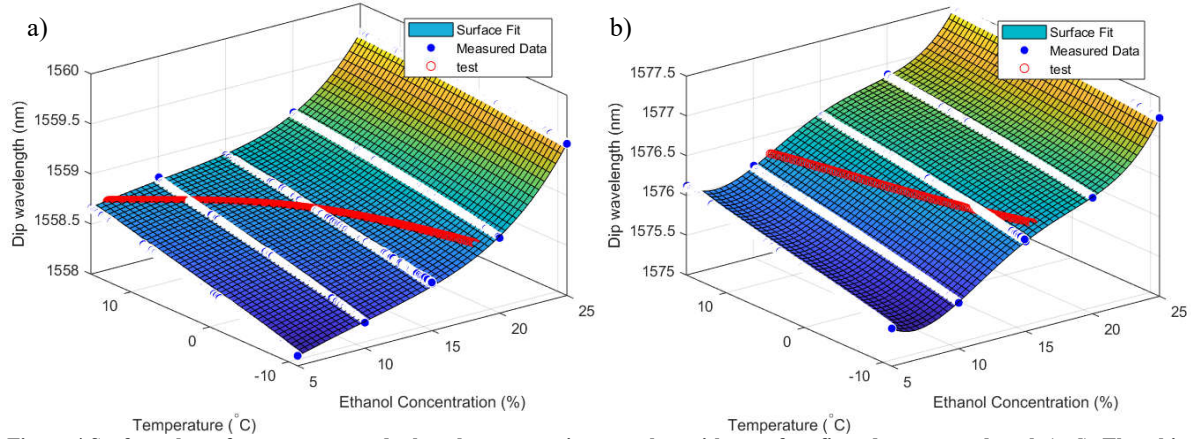


**Figure 4** Surface plots of temperature and ethanol concentration, together with a surface fit and a test wavelength (red). The white lines represent the measured data, to which a surface fit was found. A specific dip wavelength has been drawn in (contour line, red), which are plotted together in Figure 5.

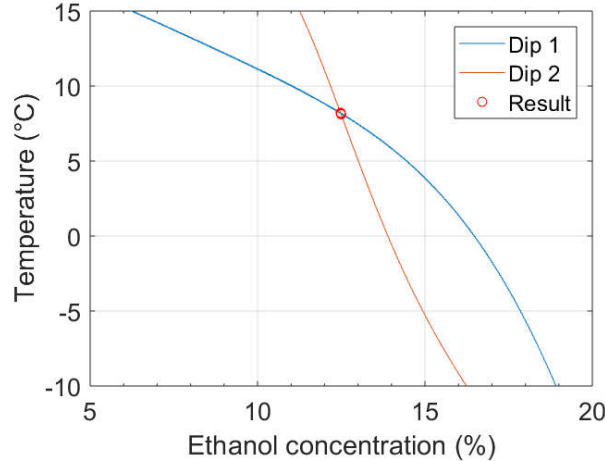


**Figure 5** Contour lines from the surface fits in Figure 4, used to find both the temperature and the ethanol concentration.

The temperature sensitivity decreases with increasing concentration of ethanol, the average sensitivities are summarized in Table 1. With approximately 18 nm spacing between the two dips, the difference in sensitivity is surprisingly large. This may be due to weakly excited cladding modes that modulates the interference pattern from the main cladding modes, as discussed in [3].

**Table 1** Average temperature sensitivities at different ethanol concentrations for the two dips ( $\lambda_1, \lambda_2$ ) in pm/K.

| T-sensitivity | 5%   | 10%  | 15%  | 20%  | 25%  |
|---------------|------|------|------|------|------|
| $\lambda_1$   | 21.7 | 21.2 | 15.8 | 13.9 | 9.02 |
| $\lambda_2$   | 25.3 | 22.7 | 18.4 | 16.7 | 9.76 |

#### 4. Conclusion

A combined temperature and refractive index sensor has been evaluated through temperature scans in various ethanol concentrations. The simple fabrication method and the reflection mode operation create a robust sensor that easily can be inserted into different media. Based on the non-constant sensitivities with regards to both temperature and ethanol concentration a method was developed to extract both parameters individually despite the cross-sensitivity. The method cross-correlates the different responses of two interference dips by finding contour lines in calibration plots. This paper focused on the simultaneous measurement of temperature and ethanol concentration, but based on the operating principle the change in RI associated with a phase transition also enables it to be detected. Further work includes improving the accuracy of the calibration measurements and generalizing the method to measure refractive index directly.

## 5. References

- [1] P. Pedevilla, M. Fitzner, and A. Michaelides, "What Makes a Good Descriptor for Heterogeneous Ice Nucleation on OH-Patterned Surfaces," pp. 25–29, 2017.
- [2] W. C. Wong *et al.*, "Miniature pH optical fiber sensor based on waist-enlarged bitaper and mode excitation," *Sensors Actuators, B Chem.*, vol. 191, pp. 579–585, 2014.
- [3] R. Xiong *et al.*, "Simultaneous measurement of refractive index and temperature based on modal interference," *IEEE Sens. J.*, vol. 14, no. 8, pp. 2524–2528, 2014.
- [4] X. Zhou, K. Chen, X. Mao, W. Peng, and Q. Yu, "A reflective fiber-optic refractive index sensor based on multimode interference in a coreless silica fiber," *Opt. Commun.*, vol. 340, pp. 50–55, 2015.
- [5] T. H. Xia, A. P. Zhang, B. Gu, and J. J. Zhu, "Fiber-optic refractive-index sensors based on transmissive and reflective thin-core fiber modal interferometers," *Opt. Commun.*, vol. 283, no. 10, pp. 2136–2139, 2010.
- [6] B. Gu, M.-J. Yin, a P. Zhang, J.-W. Qian, and S. He, "Low-cost high-performance fiber-optic pH sensor based on thin-core fiber modal interferometer," *Opt. Express*, vol. 17, no. 25, pp. 22296–22302, 2009.
- [7] L. Li, L. Xia, Z. Xie, L. Hao, B. Shuai, and D. Liu, "In-line fiber Mach-Zehnder interferometer for simultaneous measurement of refractive index and temperature based on thinned fiber," *Sensors Actuators, A Phys.*, vol. 180, pp. 19–24, 2012.
- [8] R. C. Kamikawachi *et al.*, "Determination of thermo-optic coefficient in liquids with fiber Bragg grating refractometer," *Opt. Commun.*, vol. 281, no. 4, pp. 621–625, 2008.
- [9] Y. Saito, J. J. Wang, D. A. Smith, and D. N. Batchelder, "A simple chemical method for the preparation of silver surfaces for efficient SERS," *Langmuir*, vol. 18, no. 8, pp. 2959–2961, 2002.